

Solar Sector Structure: Fact or Fiction?

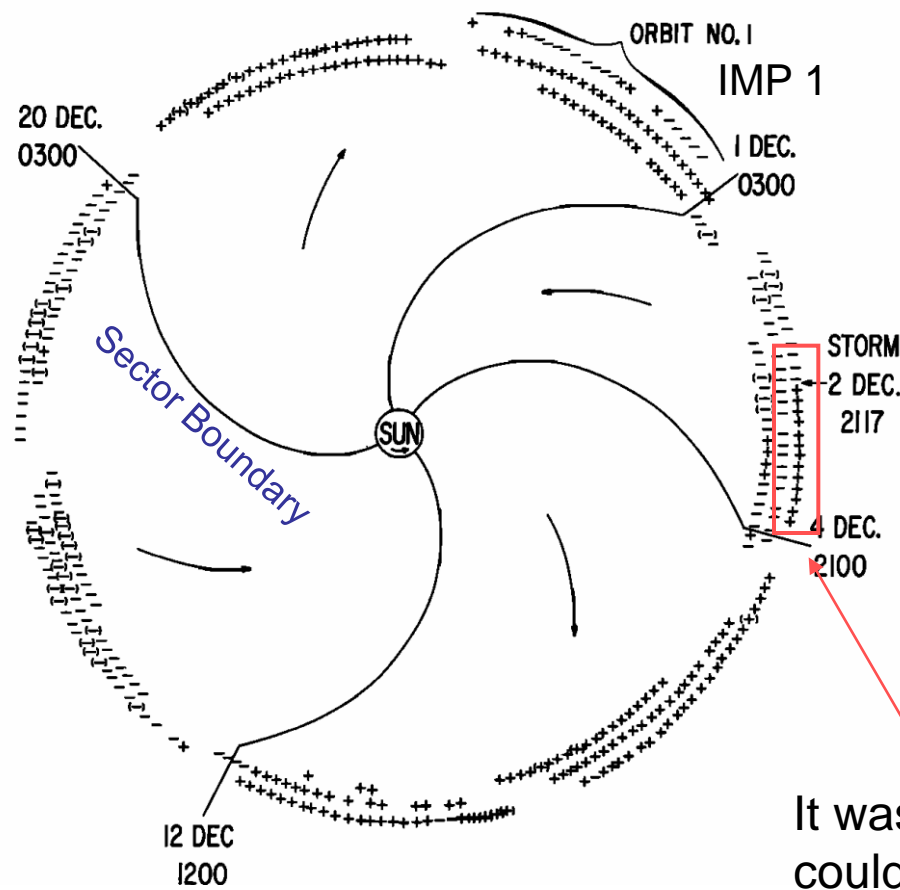
Leif Svalgaard
Stanford University

LMSAL, August 18, 2011

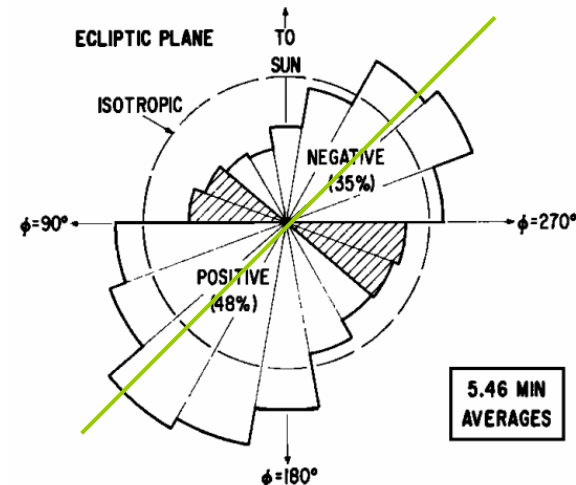
Discovery of Sector Structure

Quasi-Stationary Corotating Structure in the Interplanetary Medium

John M. Wilcox & Norman F. Ness (1965), JGR, 70, 5793.



The large-scale structuring of the IMF was a surprise at the time



It was also noted that solar storms could briefly disrupt the structure

The Structure Organizes Solar Wind Properties and Responses to those

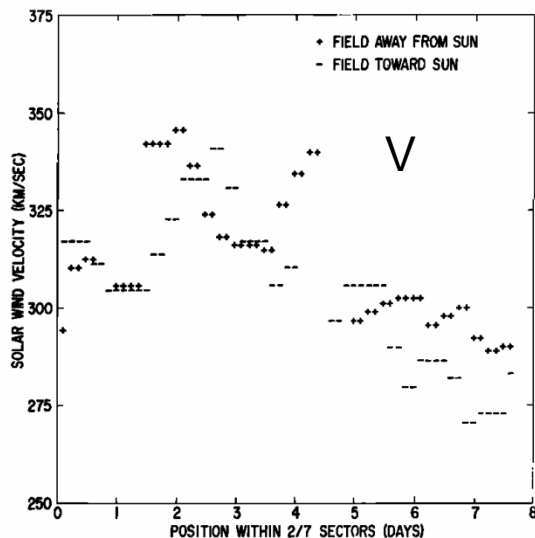


Fig. 8. Superposed epoch analysis of the solar wind velocity as a function of position within the 2/7 sectors.

Solar Wind High-speed Stream

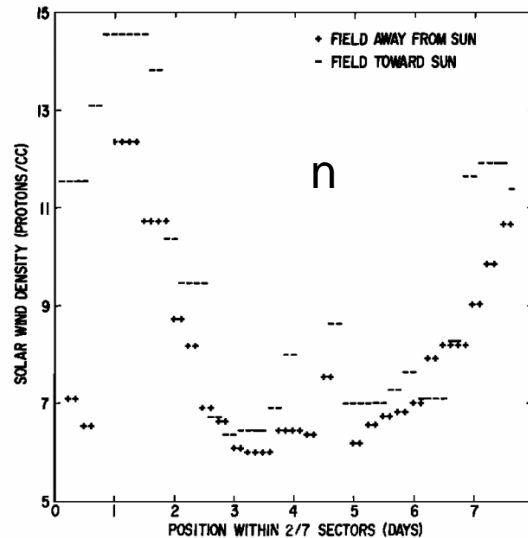


Fig. 9. Superposed epoch analysis of the solar wind density as a function of position within the 2/7 sectors.

Density Spike

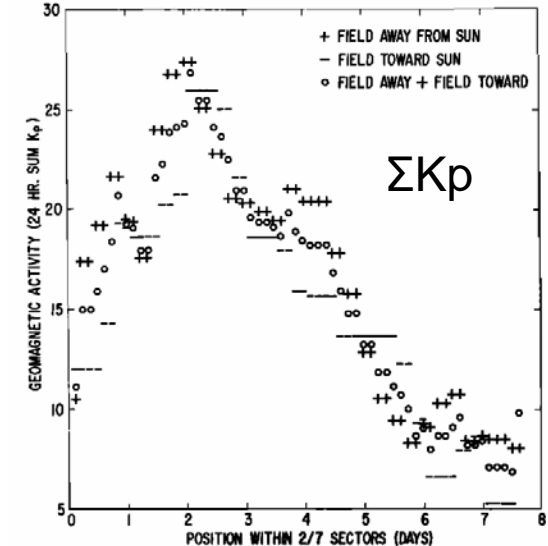
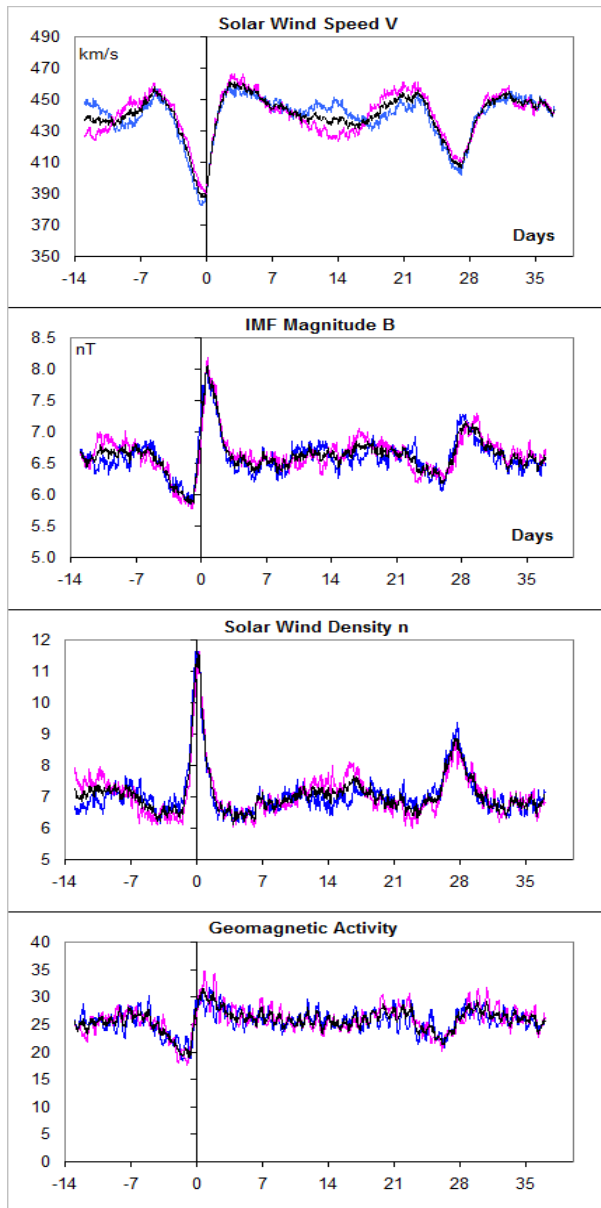


Fig. 11. Superposed epoch analysis of the geomagnetic activity index 24-hour sum K_p , as a function of position within the 2/7 sectors.

Geomagnetic Activity

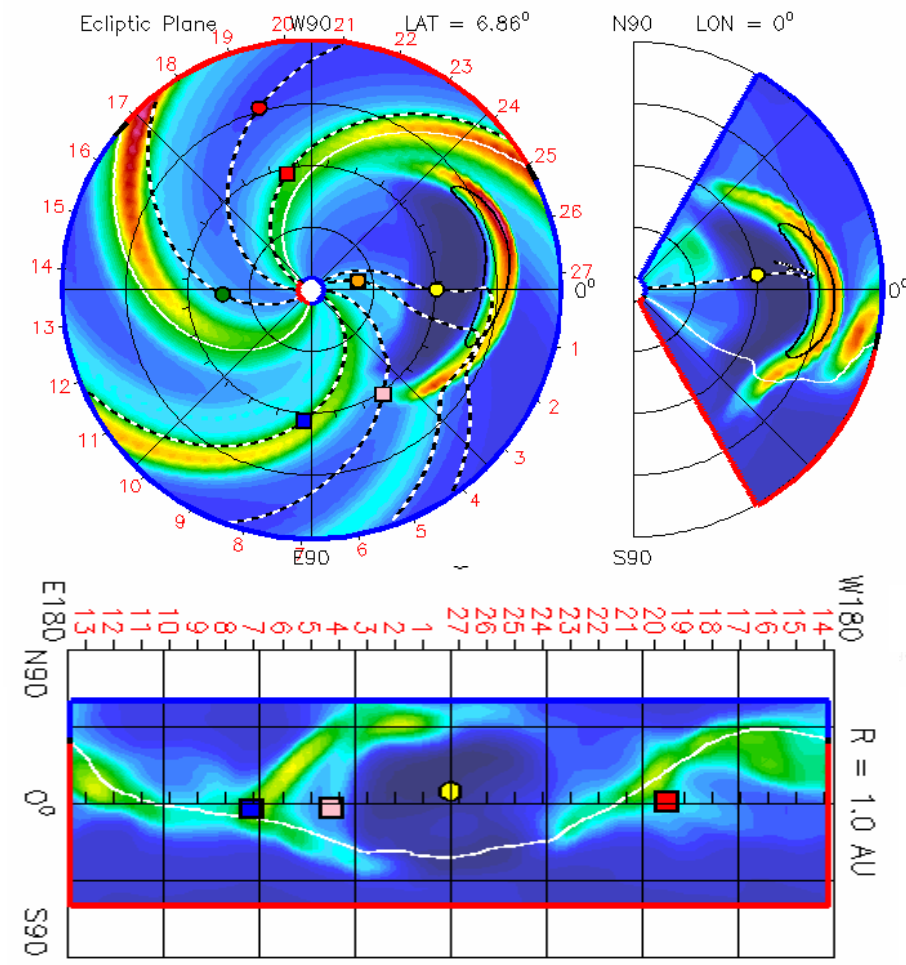
Also: Cosmic Ray Intensity, IMF Strength, Flares, UV Flux, Green Corona, etc. Almost anything was later claimed by people to be organized by the structure: Weather, Agitation of Inmates in Mental Institutions, etc. Like Global Warming today causes everything...



Organization is Robust (Co-rotating Interaction Regions)

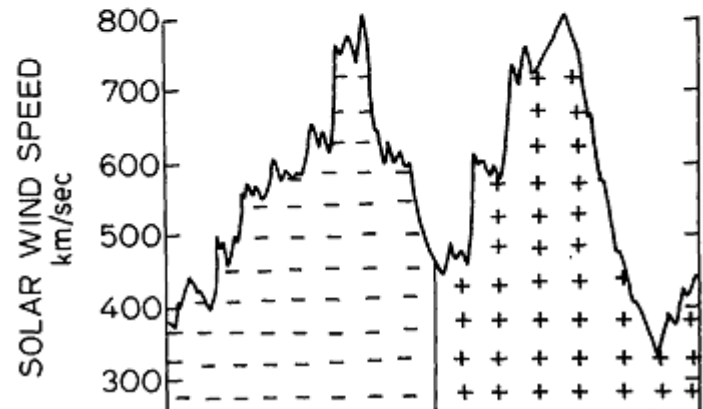
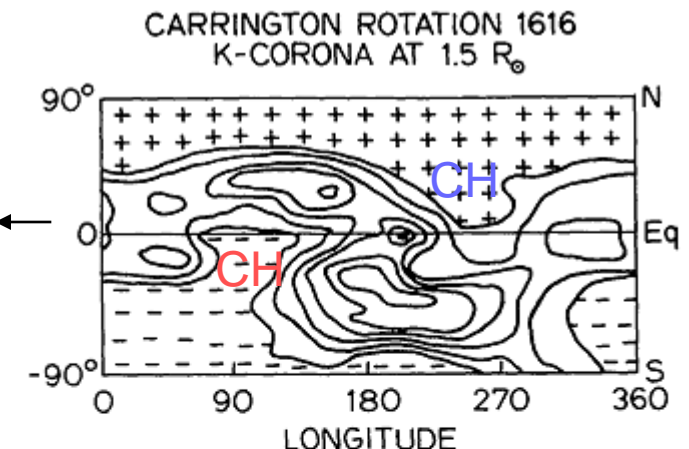
2011-08-20T18:00

● Earth ● Mars ● Mercury ● Venus ● Messenger ■ Spitzer



Superposed Epoch ~1000 Boundaries

Rotation Plots of the Sector Polarity

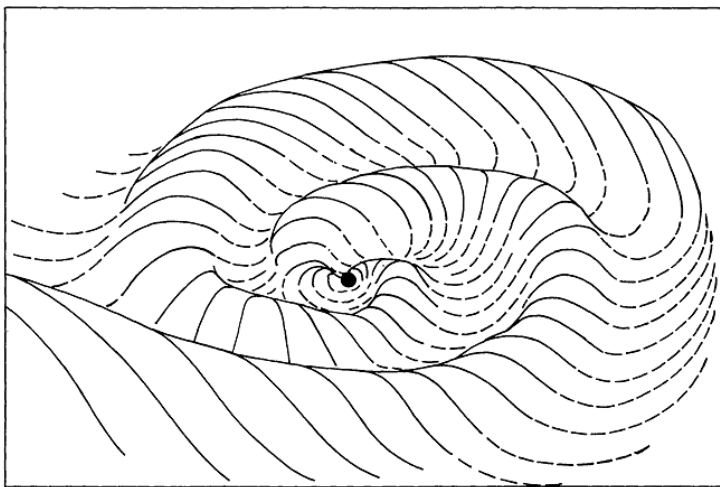
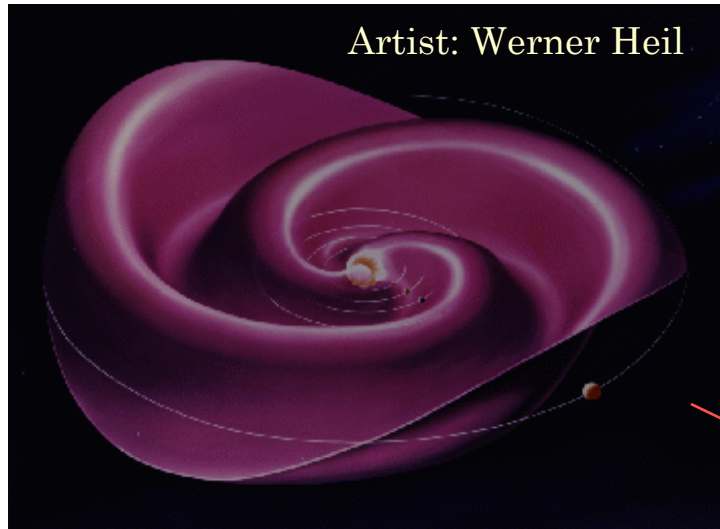


Skylab Workshop, 1976

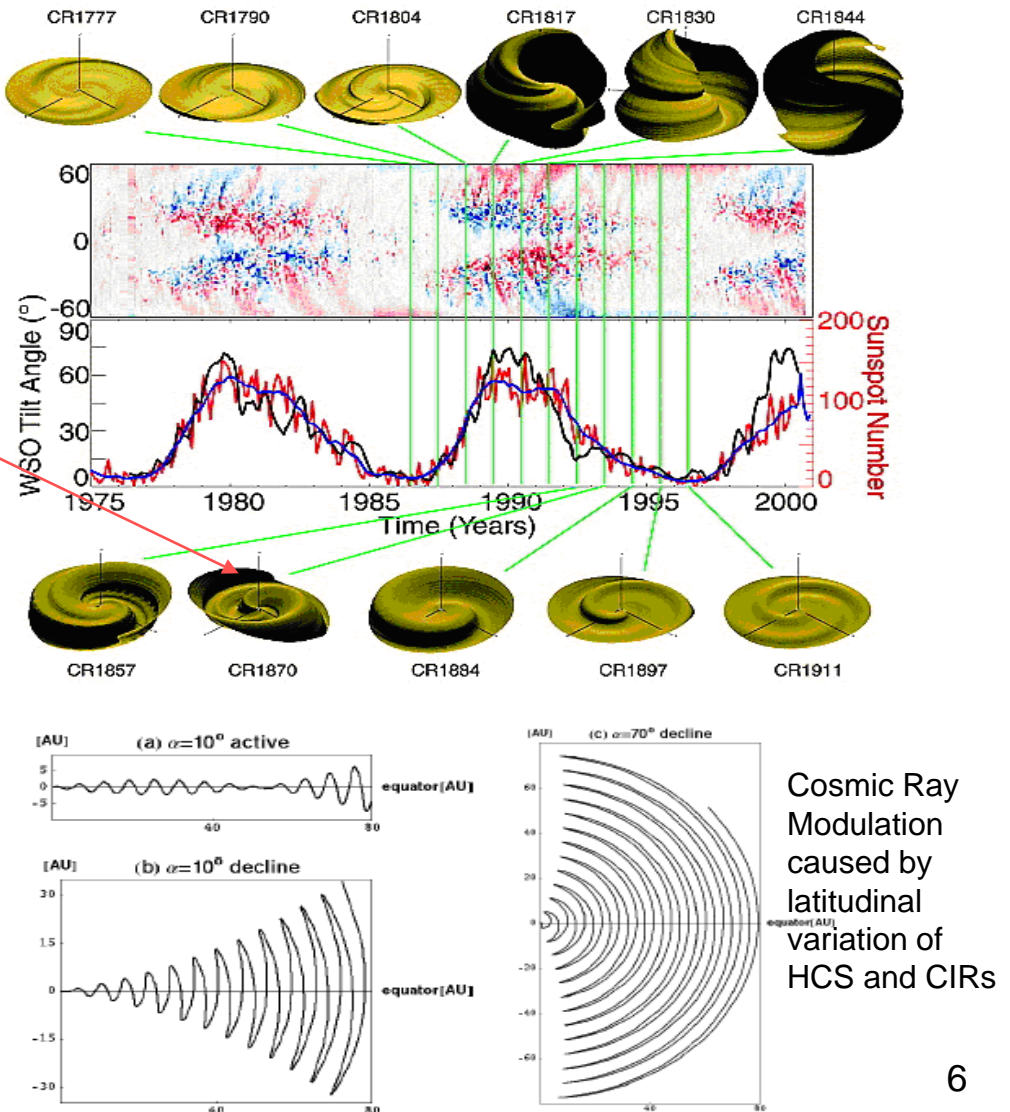
Bartels Rotations

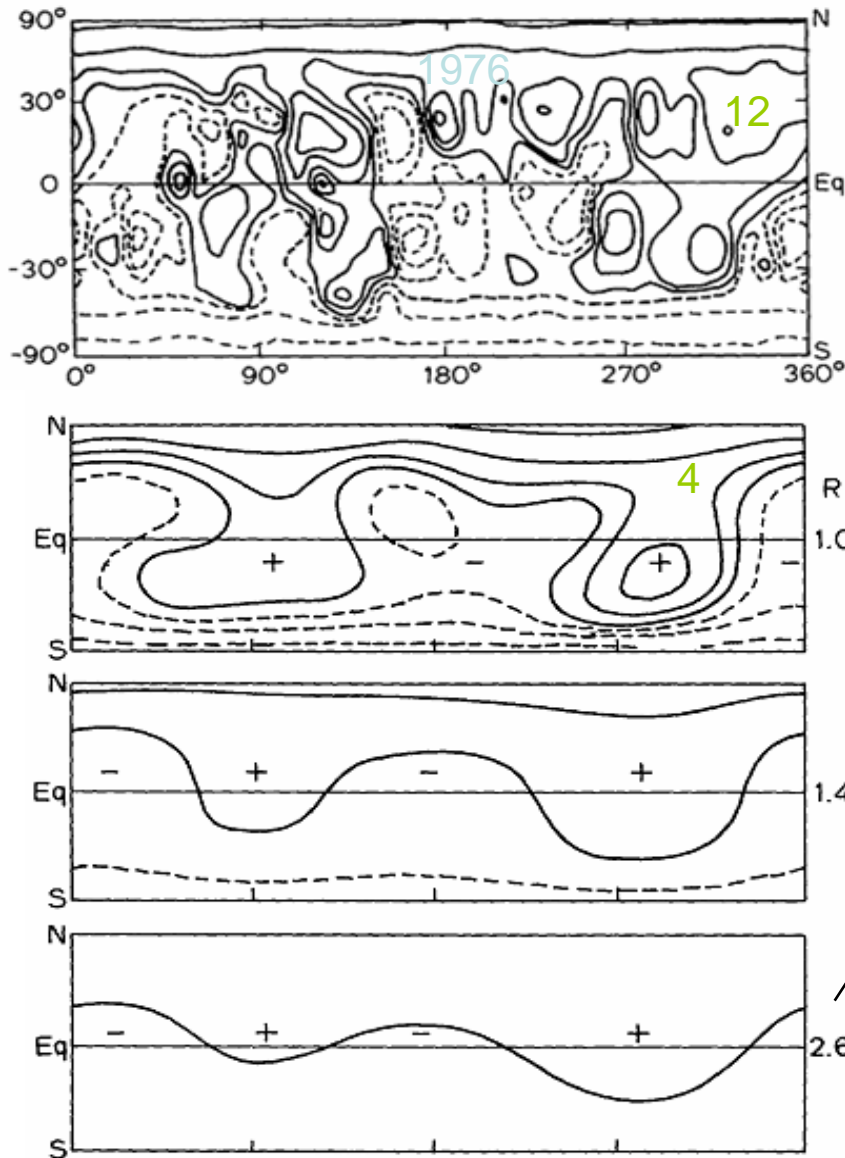
R9	Rot- No	1st day	C9	IMF POLARITY
455	422	442		1906
..	236	623	19	1907
332	326	531	1908	1908
334	565	421	73	1909
1970	M29	777	665 426 376	1910
255	235	421	11 A19	1911
344	421	33	12 M16	1912
323	544	324	13 J12	1913
3	221	222	14 J9	1914
33	..	225	15 A5	1915
775	552	225	16 S1	1916
552	22	2	17 S28	1917
452	2	2	18 025	1918
345	3	222	19 N21	1919
346	3	224	2020 A18	1920
354	2	2	19 J14	1921
334	322	2	F10 466 52	1922
323	322	222	M9 666 424	1923
345	423	222	A5 565 426 5	1924
666	42	2	M2 566 6 423	1925
354	52	2	M29 666 555	1926
364	224	2	21 125 777 652	1927
463	320	456	J22 555 653	1928
321	224	5	29 A18	1929
355	226	67	30 S16	1930
643	222	222	31 O17	1931
32	323	2	32 N7 556 777 652	1932
323	323	3	D4 555 555 524	1933
322	32	2	33 031	1934
665	22	2	19 J27	1935
665	22	2	F23 645 2 3 523	1936
1987	M22	62 6 65	38 A18	1937
223	22	2	39 M15 645 322	1938
1222	40 J11	62 324 333	40 J18	1939
323	322	223	41 52 443 442	1940
665	22	2	42 A4 62 444	1941
67	22	2	43 A31 52 561 523	1942
222	22	2	44 S27 645 2 32	1943
65	22	23	45 026 223 52	1944
221	22	2	46 N20 57 444	1945
1	22	2	1947 D17 223 5 566 423	1946
19	19	19	19 J13 223 225 655 2	1947
4	33	19	F9 62 455 4 565 26	1948
..	19	19	M7 66666 244 556 22	1949
1951	A3 766666 423 334	1950	52 A30 3 7 854	1951
52	M27 4542	1952	53 M27 4542 355 23	1953
54	J23 455	1954	55 J20	1955
55	A16	1956	56 A16	1956
57	S12	1957	57 S12	1957
58	09	1958	58 09	1958
59	NS	1959	59 NS	1959
60	O2	1960	60 2542 324	1960
61	29	1961	61 324 323 45 52	1961
62	J25	1962	62 446 523 5	1962
63	F21	1963	63 543	1963
64	M20	1964	64 423 4 44	1964
65	A16	1965	65 76	1965
66	M13	1966	66 4553	1966
67	J9	1967	67 4554	1967
68	16	1968	68 765 543 35 64	1968
69	binary	1969	69 prel-	1969
70	765 543	1970	70 765 543	1970
71	765 543	1971	71 765 543	1971
72	765 543	1972	72 765 543	1972
73	765 543	1973	73 765 543	1973
74	765 543	1974	74 765 543	1974
75	765 543	1975	75 765 543	1975
76	765 543	1976	76 765 543	1976
77	765 543	1977	77 765 543	1977
78	765 543	1978	78 765 543	1978
79	765 543	1979	79 765 543	1979
80	765 543	1980	80 765 543	1980
81	765 543	1981	81 765 543	1981
82	765 543	1982	82 765 543	1982
83	765 543	1983	83 765 543	1983
84	765 543	1984	84 765 543	1984
85	765 543	1985	85 765 543	1985
86	765 543	1986	86 765 543	1986
87	765 543	1987	87 765 543	1987
88	765 543	1988	88 765 543	1988
89	765 543	1989	89 765 543	1989
90	765 543	1990	90 765 543	1990
91	765 543	1991	91 765 543	1991
92	765 543	1992	92 765 543	1992
93	765 543	1993	93 765 543	1993
94	765 543	1994	94 765 543	1994
95	765 543	1995	95 765 543	1995
96	765 543	1996	96 765 543	1996
97	765 543	1997	97 765 543	1997
98	765 543	1998	98 765 543	1998
99	765 543	1999	99 765 543	1999
100	765 543	2000	100 765 543	2000
101	765 543	2001	101 765 543	2001
102	765 543	2002	102 765 543	2002
103	765 543	2003	103 765 543	2003
104	765 543	2004	104 765 543	2004
105	765 543	2005	105 765 543	2005
106	765 543	2006	106 765 543	2006
107	765 543	2007	107 765 543	2007
108	765 543	2008	108 765 543	2008
109	765 543	2009	109 765 543	2009
110	765 543	2010	110 765 543	2010
111	765 543	2011	111 765 543	2011
112	765 543	2012	112 765 543	2012
113	765 543	2013	113 765 543	2013
114	765 543	2014	114 765 543	2014
115	765 543	2015	115 765 543	2015
116	765 543	2016	116 765 543	2016
117	765 543	2017	117 765 543	2017
118	765 543	2018	118 765 543	2018
119	765 543	2019	119 765 543	2019
120	765 543	2020	120 765 543	2020
121	765 543	2021	121 765 543	2021
122	765 543	2022	122 765 543	2022
123	765 543	2023	123 765 543	2023
124	765 543	2024	124 765 543	2024
125	765 543	2025	125 765 543	2025
126	765 543	2026	126 765 543	2026
127	765 543	2027	127 765 543	2027
128	765 543	2028	128 765 543	2028
129	765 543	2029	129 765 543	2029
130	765 543	2030	130 765 543	2030
131	765 543	2031	131 765 543	2031
132	765 543	2032	132 765 543	2032
133	765 543	2033	133 765 543	2033
134	765 543	2034	134 765 543	2034
135	765 543	2035	135 765 543	2035
136	765 543	2036	136 765 543	2036
137	765 543	2037	137 765 543	2037
138	765 543	2038	138 765 543	2038
139	765 543	2039	139 765 543	2039
140	765 543	2040	140 765 543	2040
141	765 543	2041	141 765 543	2041
142	765 543	2042	142 765 543	2042
143	765 543	2043	143 765 543	2043
144	765 543	2044	144 765 543	2044
145	765 543	2045	145 765 543	2045
146	765 543	2046	146 765 543	2046
147	765 543	2047	147 765 543	2047
148	765 543	2048	148 765 543	2048
149	765 543	2049	149 765 543	2049
150	765 543	2050	150 765 543	2050
151	765 543	2051	151 765 543	2051
152	765 543	2052	152 765 543	2052
153	765 543	2053	153 765 543	2053
154	765 543	2054	154 765 543	2054
155	765 543	2055	155 765 543	2055

The Heliospheric Current Sheet



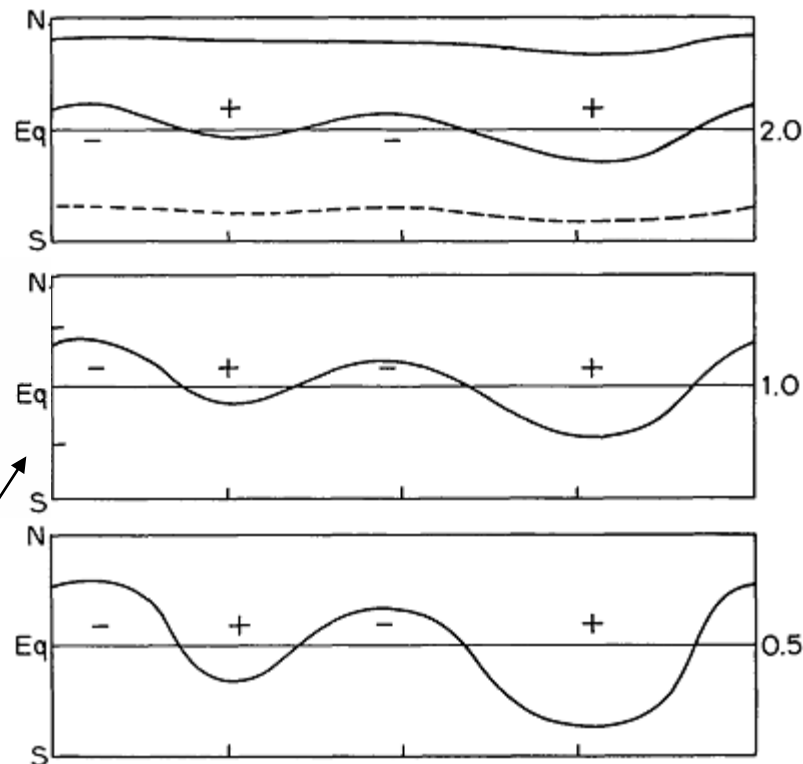
Svalgaard & Wilcox, *Nature*, 1976





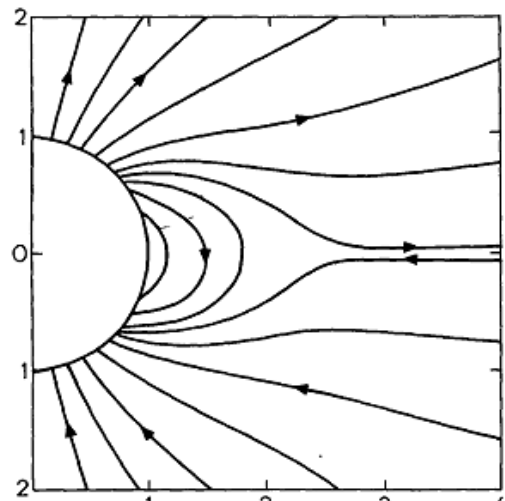
Simplification and Flattening with Height
“Domes of closed field lines”

The Potential Field Source Surface Model Illustrates Many First-Order Effects

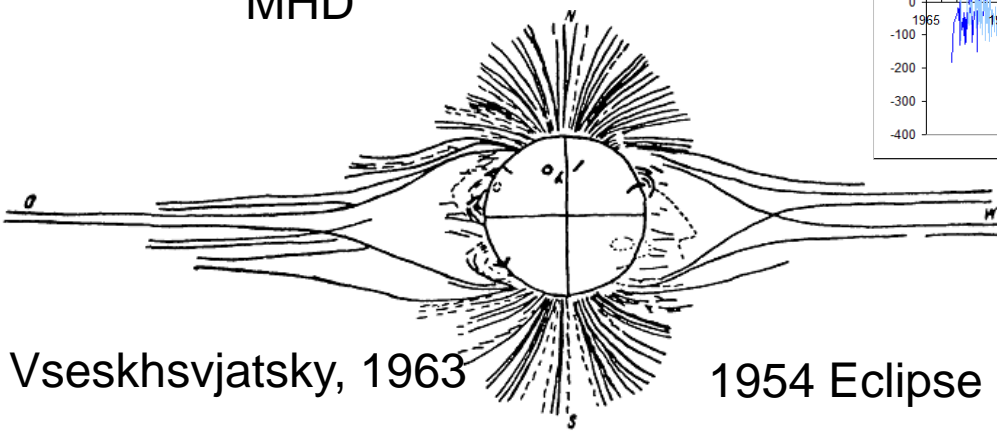


Flattening with Polar Fields

The Importance of the Polar Fields



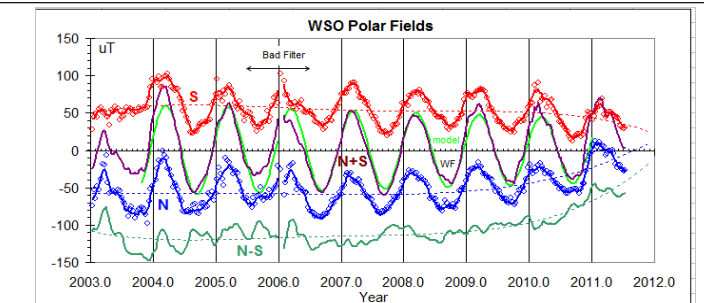
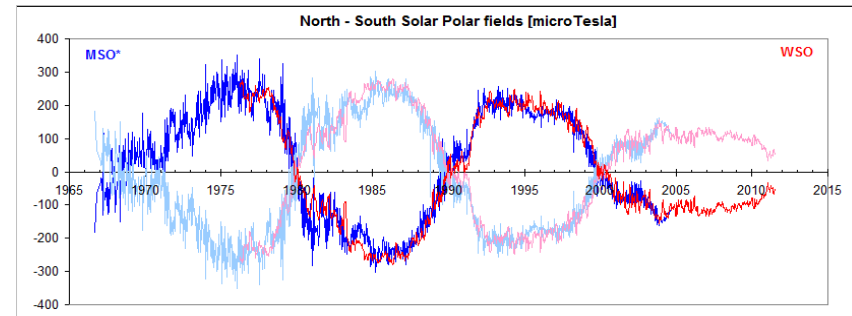
Pneuman & Kopp, 1971
MHD



Vseskhsvjatsky, 1963
1954 Eclipse

Even with all the sophistication of current models of the Corona and HMF they are hostage to the correct value of the solar polar fields, which may be different at the two poles and even have longitudinal structure within the polar caps.

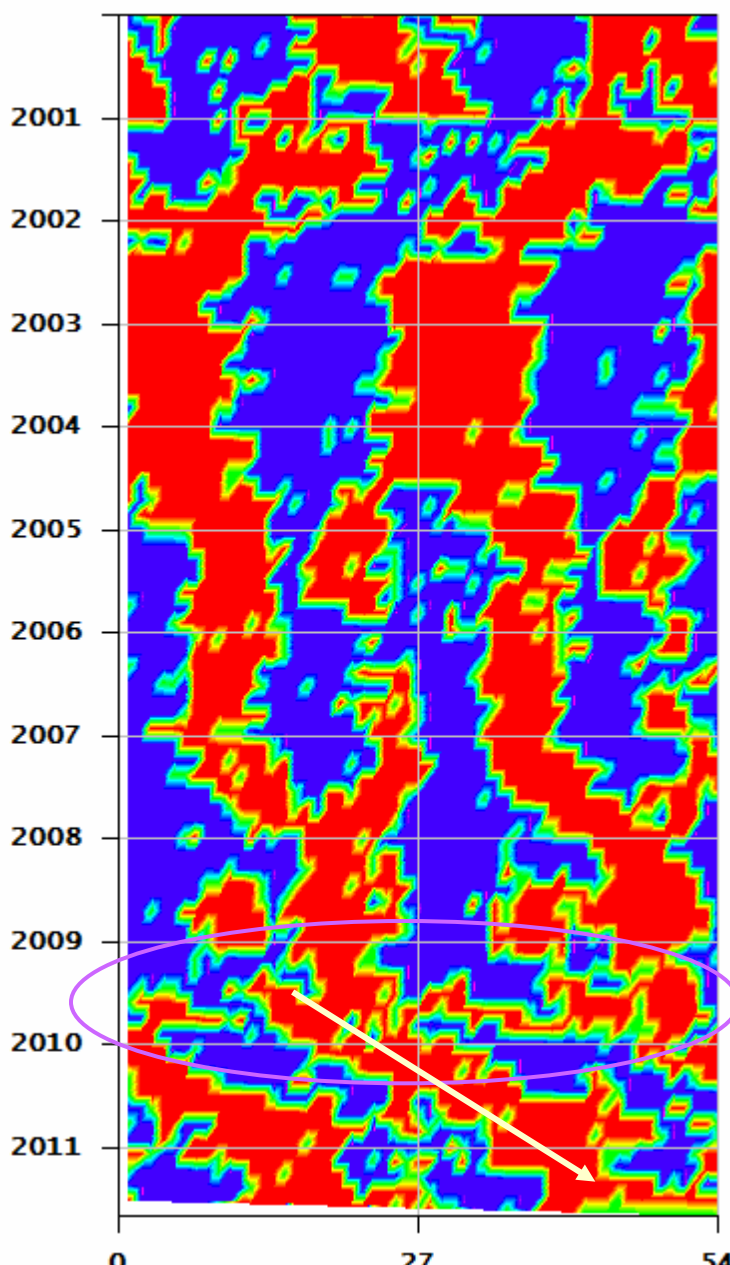
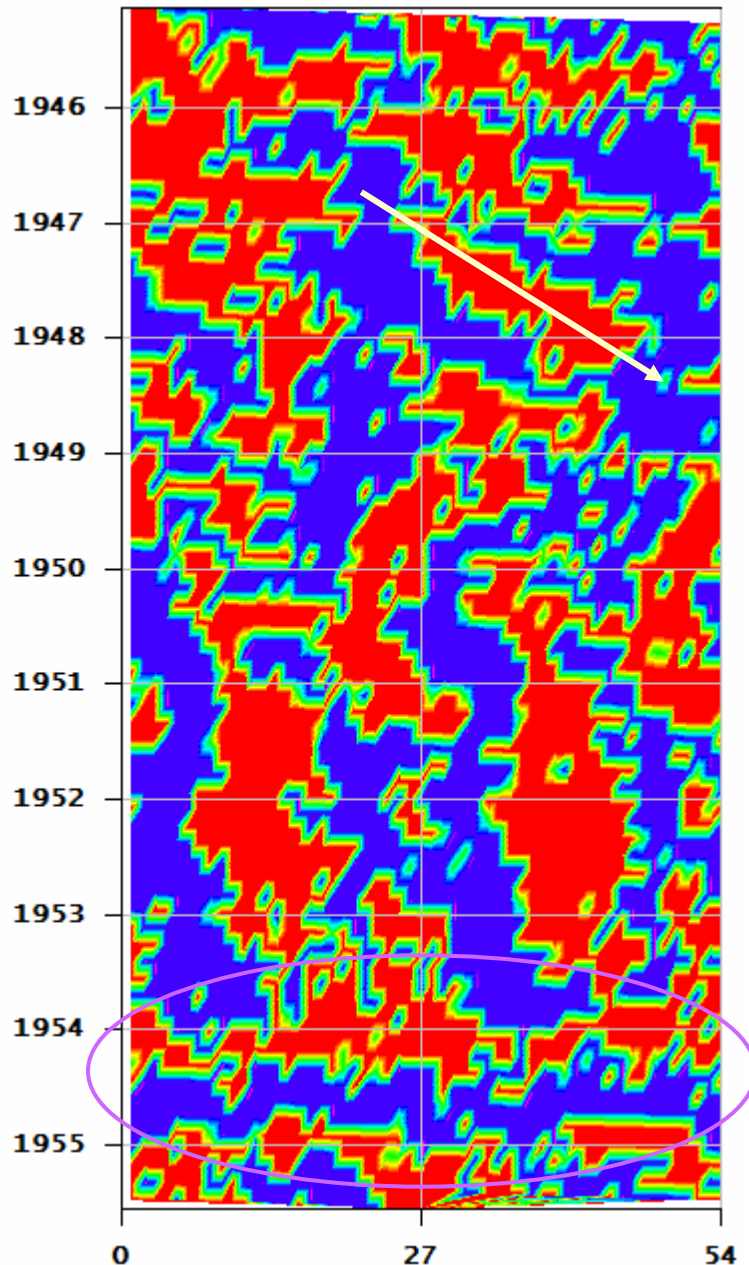
This is particularly important at solar minimum when the HCS is largely flat.



Rotation Plots of Polarity

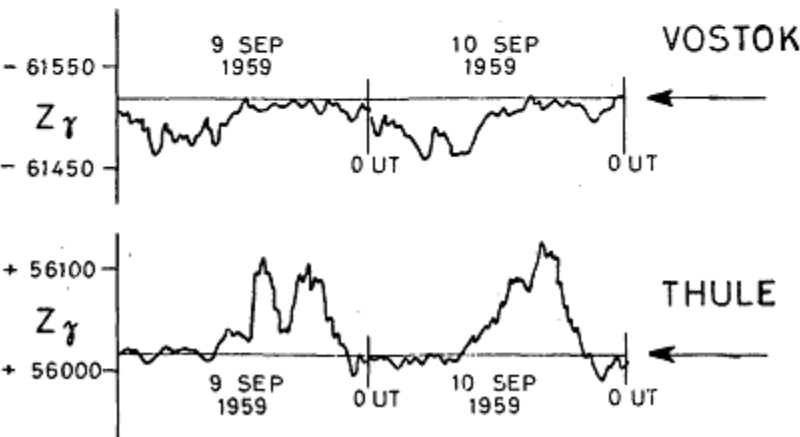
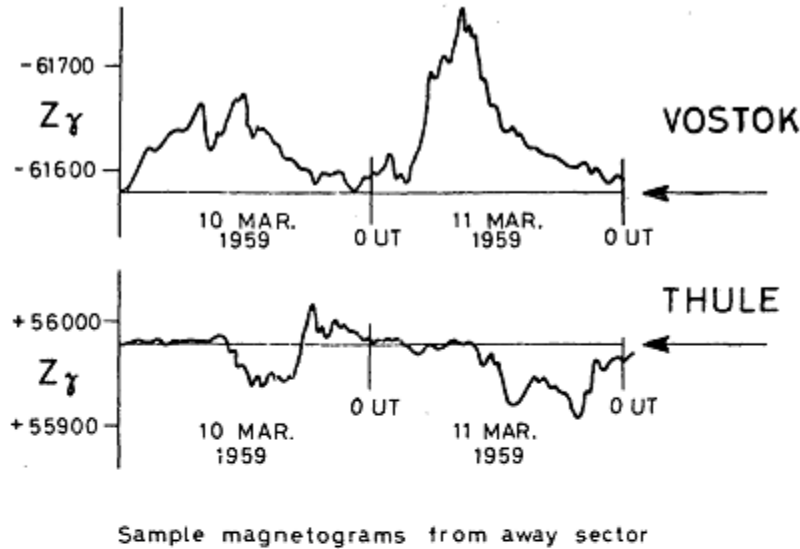
Recurrent for years

- Towards, -
- Away, +



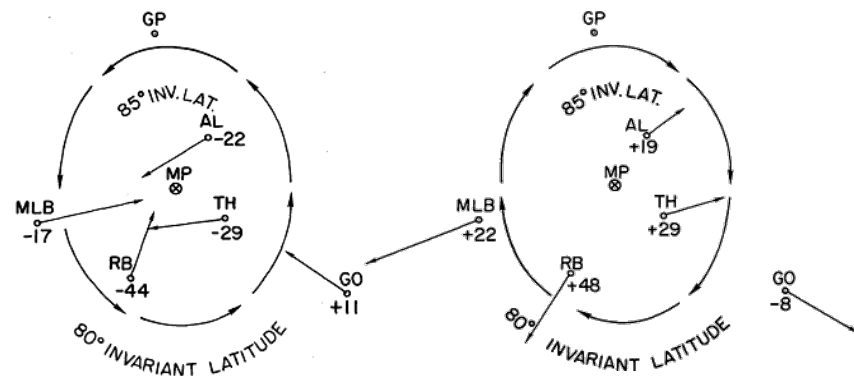
In 1954 the HCS was so flat that the Earth was above the sheet for six months at a time

Rosenberg-Coleman Effect



How do we know the Sector Polarity Before the Space age?

The HMF reconnects with the Earth's magnetic field and deforms it depending on the sign of the HMF. This creates an electric current vortex, whose magnetic effects we can measure on the ground:

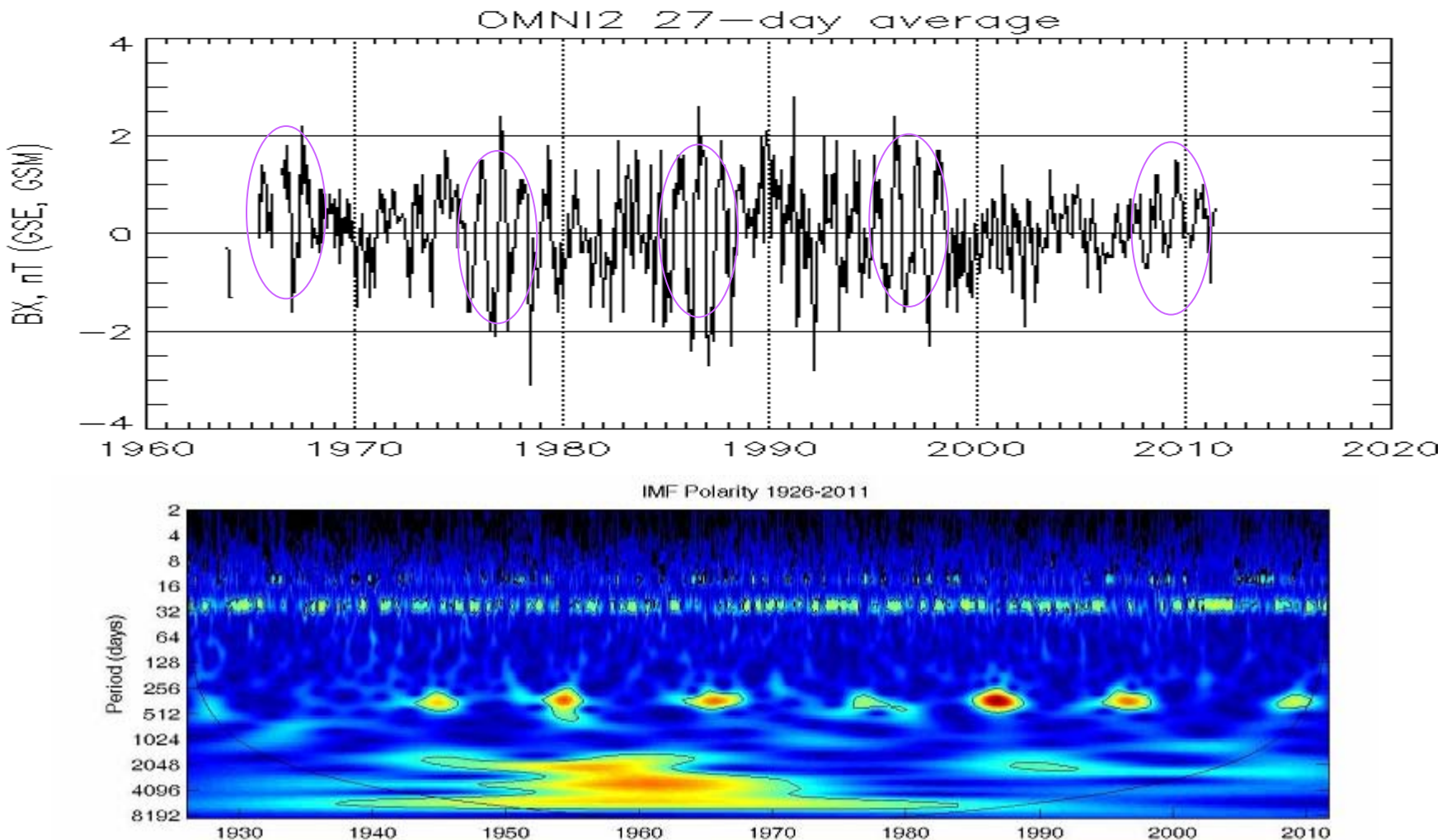


Away

Data goes back to 1926

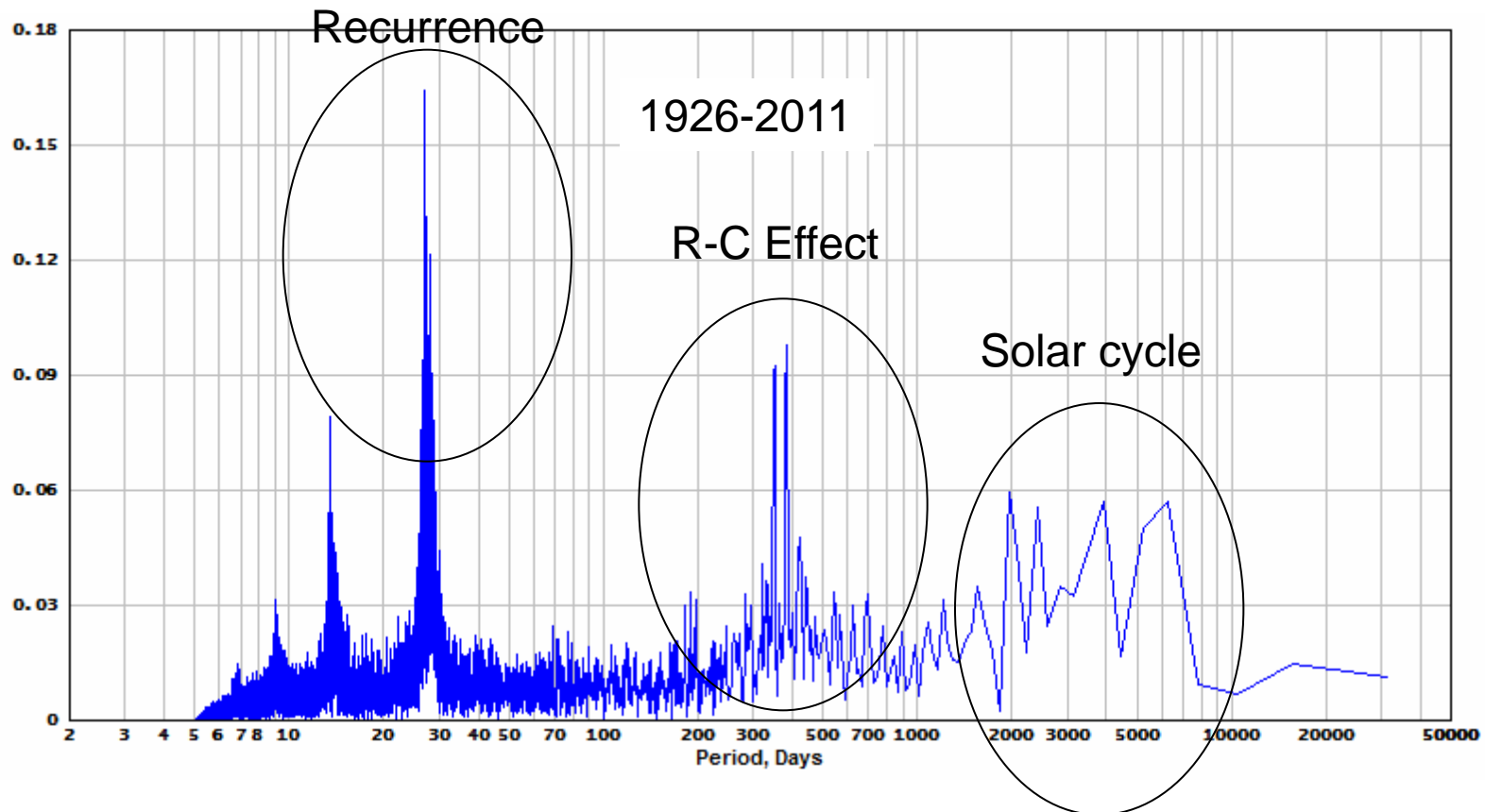
Toward

Dominant Polarity: Rosenberg-Coleman Effect



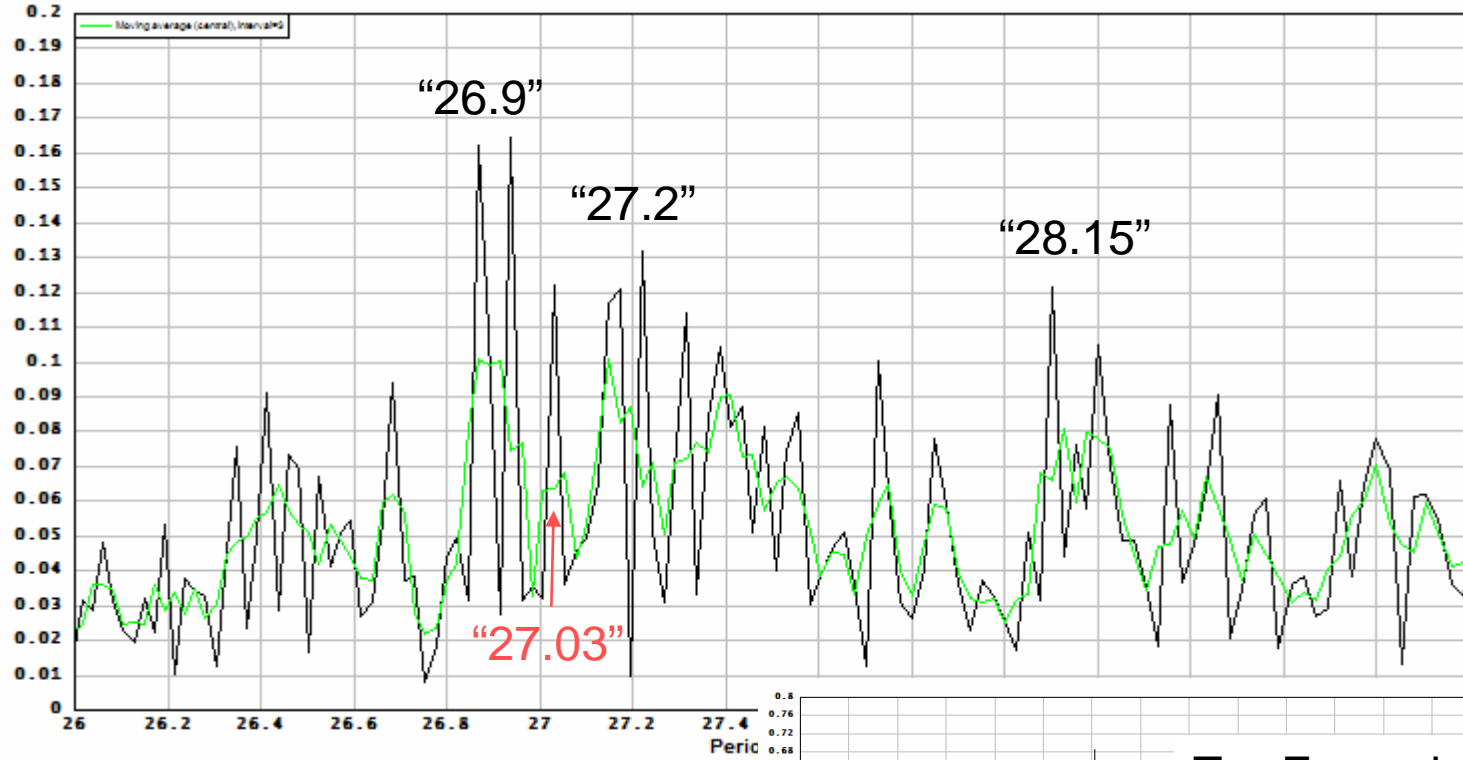
Proves Polar Field Reversals in the Past

FFT Power Spectrum of Polarity



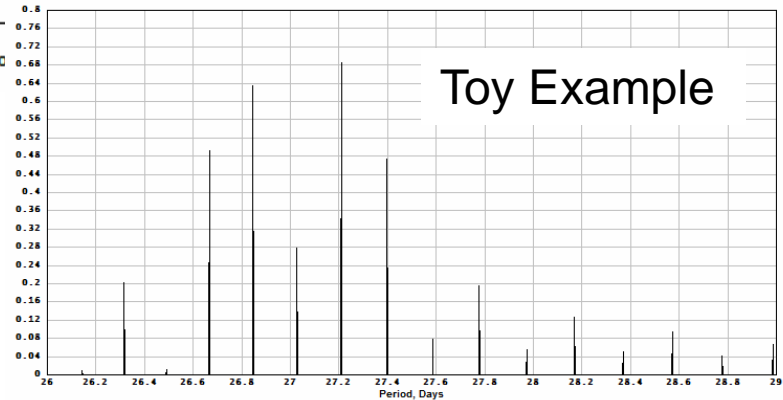
The Recurrence Line is split into several lines

Recurrence Peak: Fine Structure



The 27.03 line is an artifact having contributions from the 26.9 and 27.2 lines

Toy Example



Average Recurrence Period in Solar Wind Data

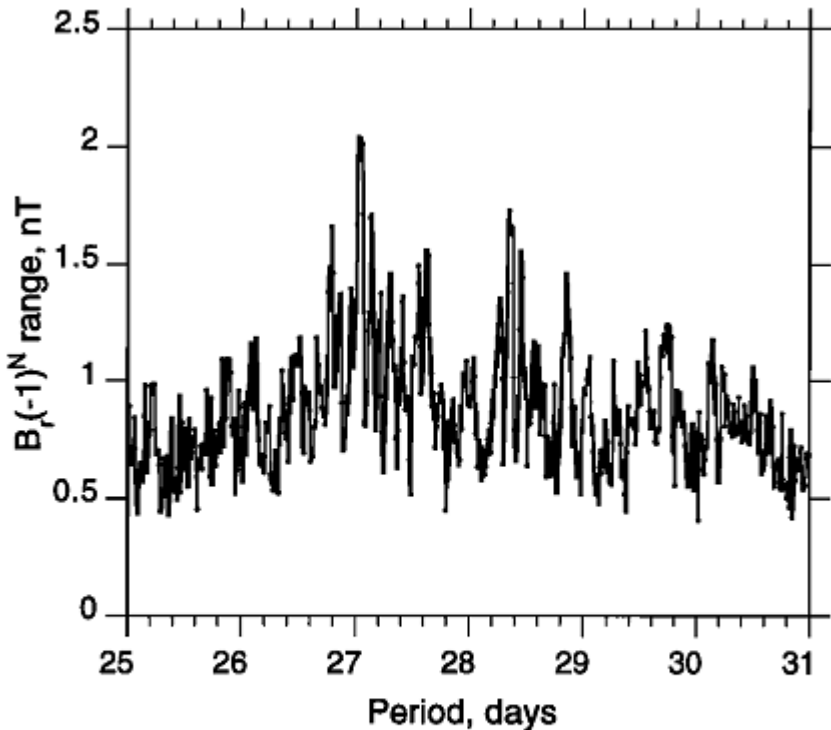
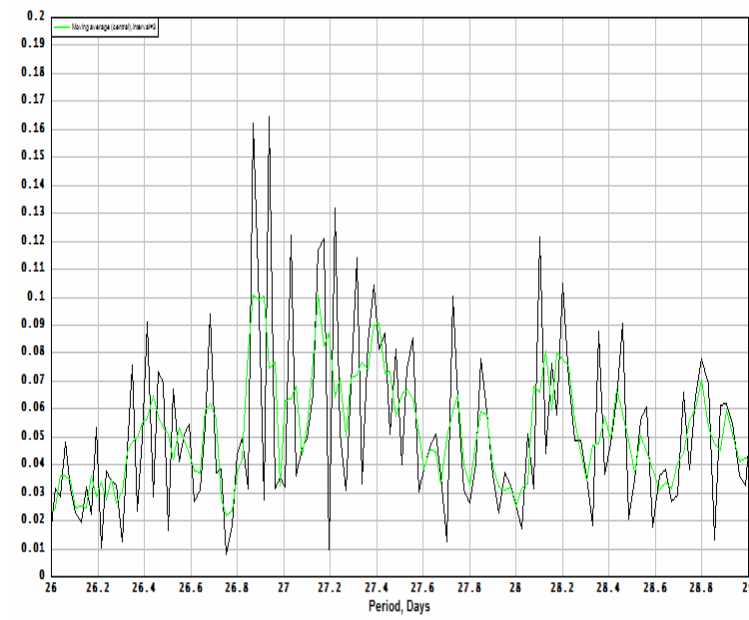
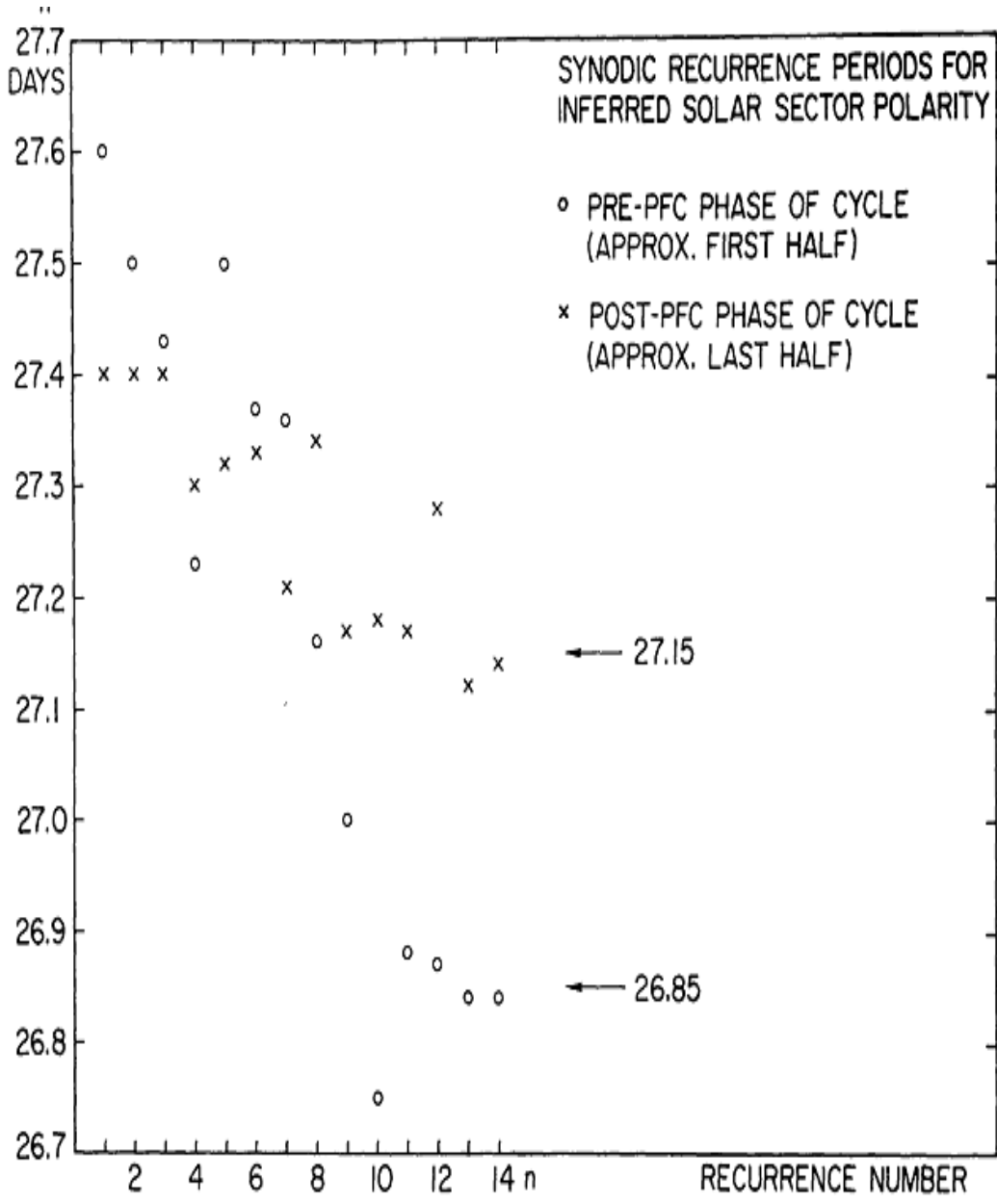


Figure 5. The difference between the highest and the lowest values of $B_r(-1)^N$ for the time-averaged $B_r(-1)^N$ versus longitude curves as a function of solar rotation period from 25 to 31 days.



"On average, solar magnetic field lines in the ecliptic plane point outward on one side of the Sun and inward on the other, reversing direction approximately every 11 years while maintaining the same phase. The data are consistent with a model in which the solar magnetic dipole returns to the same longitude after each reversal."

Neugebauer et al., 2000



Recurrence Period depends on Solar Cycle Phase

26.85 d before polar field reversal

27.15 d after polar field reversal

Autocorrelation at different
lags shows peaks at $n * P(n)$

Active Longitudes [an Example]

The Physics of Chromospheric Plasmas

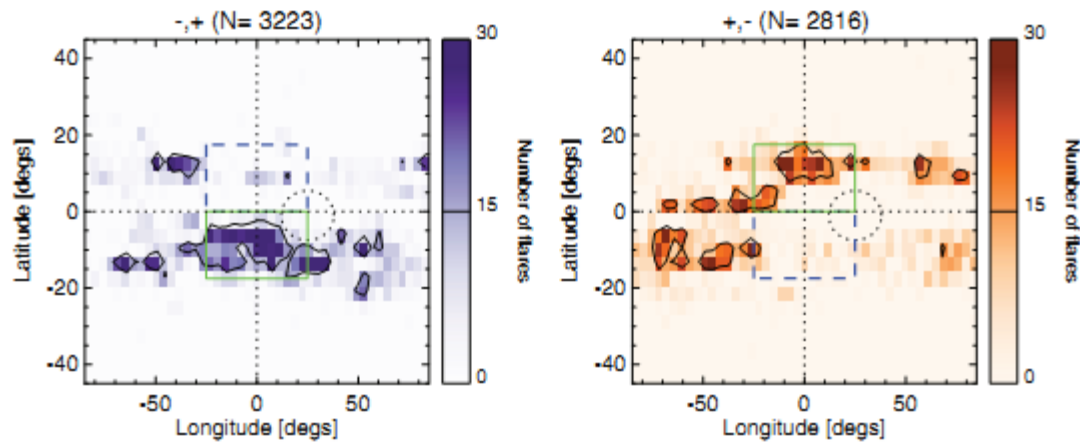
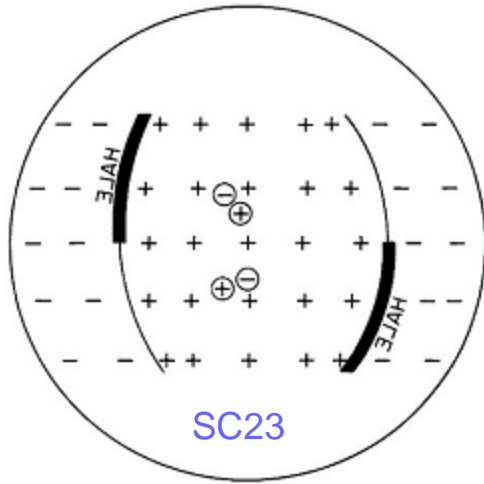
ASP Conference Series, Vol. 368, 2007

Regularities in the Distribution of Solar Magnetic Fields

V. Bumba, M. Klvána and A. Garcia

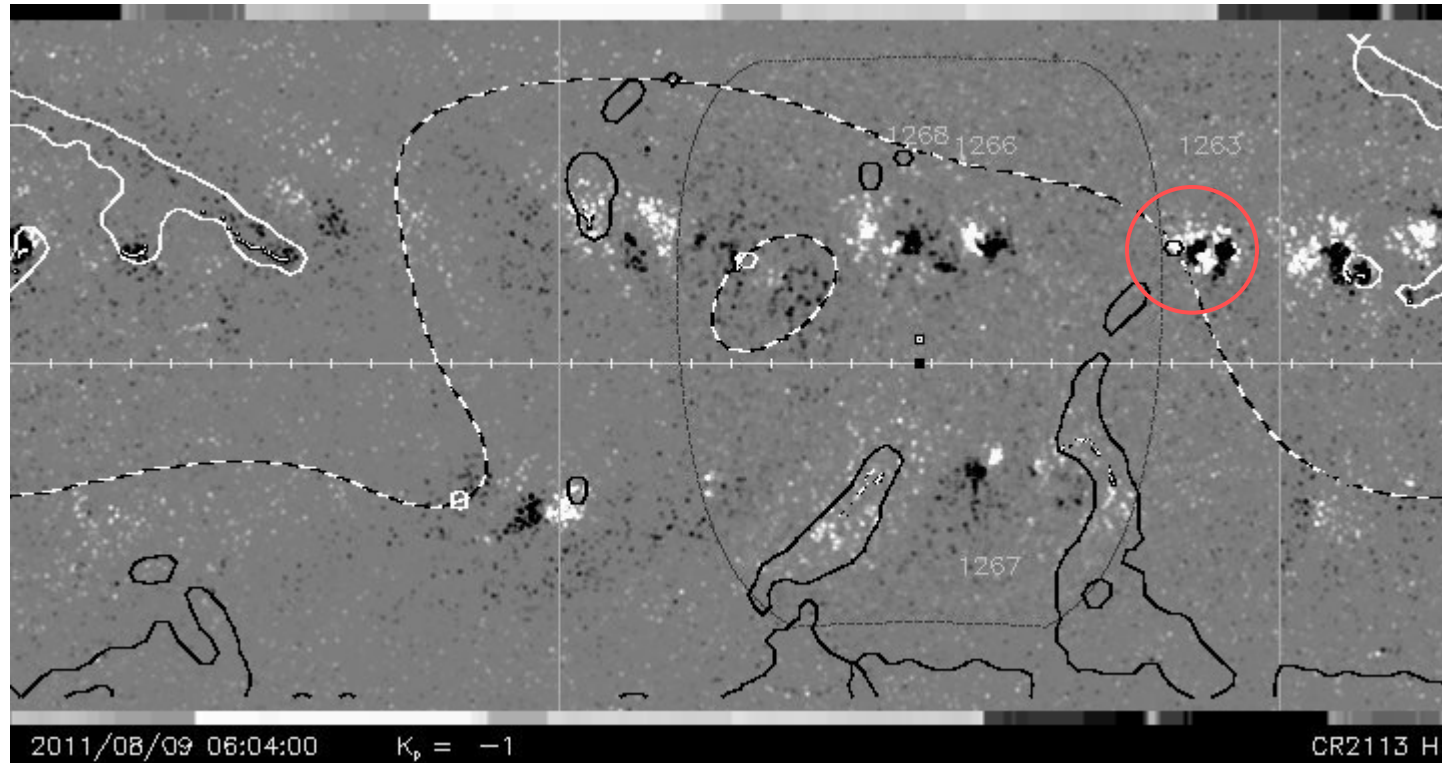
Abstract. We examined the distribution and concentration of the solar magnetic fields from the Wilcox observatory synoptic charts for the whole period of their existence (May 1976 – February 2006). We divided them into four latitudinal zones, studying the changes of their various structures, density, etc. These sets of maps demonstrate striking regularities in the photospheric magnetic field distribution with time, continuous existence of characteristic longitudes of magnetic field concentration and their longitudinal shift with three main rotational periods of **26.8**, **28.2**, and **27.14** days. They show formation of specific structures of background weaker fields, connected with the development of activity complexes, polarity alternation, etc...

Hale Boundaries and Flares



Distribution of RHESSI flares within ± 24 hr of 223 sector boundaries mapped back to central meridian (dashed vertical line) for part of solar cycle 23, 2002 March to 2008 March. The left and right panels show the $(-, +)$ and $(+, -)$ boundaries, respectively. The green boxes show where flares are expected, based on association with strong magnetic fields, i.e., at the Hale boundary. The dashed purple boxes show that hardly any flares occur near a non-Hale boundary. The number of flares in each distribution is shown above each plot. Only flares within $\pm 85^\circ$ of CM are counted. The small dashed line circles show the center of the bias area for the RHESSI imaging axis.

Recent X7 Flare on Hale Boundary



Is the magnetic field already ‘stressed’ when emerging if on a Hale Boundary? McClymont & Fisher (1989) make this case generally: the emerging flux adds stressed magnetic fields directly to the lower solar atmosphere, storing the non-potential energy needed for flaring.

The Issue

- Is the solar sector structure the result of surface flux transport of essentially randomly distributed flux?
- Or is the sector structure the result of deep-seated solar processes, resulting in longitudinal organization of the field?
- Helioseismology might discover longitudinal structures and flows (if we look for them)